Future changes in atmospheric rivers and their implications for winter flooding in Britain

David A Lavers[1,2,6], **Richard P Allan**[1,2,3], **Gabriele Villarini**[4],
Benjamin Lloyd-Hughes[2], **David J Brayshaw**[1,2,3] **and Andrew J Wade**[2,5]

[1] Department of Meteorology, University of Reading, Reading, UK
[2] Walker Institute, University of Reading, Reading, UK
[3] National Centre for Atmospheric Science, University of Reading, Reading, UK
[4] IIHR-Hydroscience and Engineering, The University of Iowa, Iowa City, IA, USA
[5] Department of Geography and Environmental Science, University of Reading, Reading, UK

E-mail: david-lavers@uiowa.edu

Abstract

Within the warm conveyor belt of extra-tropical cyclones, atmospheric rivers (ARs) are the key synoptic features which deliver the majority of poleward water vapour transport, and are associated with episodes of heavy and prolonged rainfall. ARs are responsible for many of the largest winter floods in the mid-latitudes resulting in major socioeconomic losses; for example, the loss from United Kingdom (UK) flooding in summer/winter 2012 is estimated to be about $1.6 billion in damages. Given the well-established link between ARs and peak river flows for the present day, assessing how ARs could respond under future climate projections is of importance in gauging future impacts from flooding. We show that North Atlantic ARs are projected to become stronger and more numerous in the future scenarios of multiple simulations from five state-of-the-art global climate models (GCMs) in the fifth Climate Model Intercomparison Project (CMIP5). The increased water vapour transport in projected ARs implies a greater risk of higher rainfall totals and therefore larger winter floods in Britain, with increased AR frequency leading to more flood episodes. In the high emissions scenario (RCP8.5) for 2074–2099 there is an approximate doubling of AR frequency in the five GCMs. Our results suggest that the projected change in ARs is predominantly a thermodynamic response to warming resulting from anthropogenic radiative forcing.

Keywords: atmospheric rivers, climate change, CMIP5, flooding, UK

S Online supplementary data available from stacks.iop.org/ERL/8/034010/mmedia

1. Introduction

Atmospheric rivers (ARs) describe narrow bands (around 300 km wide and 1000s of km in length) of intense moisture flux in the lower troposphere (around 1–2.5 km in altitude) which often deliver sustained and heavy rainfall to mid-latitude regions (e.g. western North America and western Europe), with associated flooding particularly in the winter half-year (October–March) [1–5]. The winter period is the focus in this letter due to the strong association between ARs and the synoptic-scale weather systems (extra-tropical 'storms' or cyclones) that are most prevalent in the winter half-year. To exemplify the large moisture transport, the AR responsible for the flooding in northwest Britain on the

[6] Present address: IIHR-Hydroscience and Engineering, The University of Iowa, Iowa City, IA, USA.

19 November 2009 had a moisture transport off the coast of northwest Britain of more than 4500 times the average gauged flow in the River Thames in London. In Britain ARs are particularly responsible for extreme floods in impermeable upland river basins in the west, and have less influence on fluvial flooding in eastern lowland basins [3].

There are two primary ways in which ARs may change in a changing climate. Firstly there may be a change in the number of ARs, which may affect the frequency of future heavy rainfall and floods. (Observed AR inter-annual variability is between about 2 and 14 events per winter [4].) This will depend on baroclinic wave activity and extra-tropical cyclones over the North Atlantic sector resulting from the spatial movement and change in characteristics of the large-scale atmospheric circulation (including the tropospheric jet). Secondly the intensity distribution of ARs could change. Mid-latitude atmospheric water vapour content in a warmer climate is expected to rise due to an increase in saturation water vapour pressure with air temperature, as governed by the Clausius–Clapeyron equation [6]; this is likely to result in increased water vapour transport, and potentially higher rainfall totals, with increasing risk of larger flood episodes.

An assessment of projections from seven climate models for California [7] suggests an increase in the number of years with high AR frequency, an increase in water vapour transport in ARs and a lengthening of the season in which ARs occur. All of the evidence in that region points towards an enhanced flood risk from ARs. In the European-oriented literature it has, however, been more commonplace to assess the location and strength of future storm tracks, with details of the flood generating AR mechanism within storms being rarely assessed. The latest storm track assessments based on climate models in the fifth Climate Model Intercomparison Project (CMIP5) [8] archive indicate that the North Atlantic winter storm track could become slightly stronger near the British Isles, both in terms of track density (number of cyclones) and average storm intensity (winds and precipitation) [9]. Broadly, this pattern of storm track change is consistent with that estimated from the cruder data available in the previous CMIP project [10]—suggestive of dynamical changes in both the synoptic- and large-scale flow [11].

Here, we investigate directly for the first time how the characteristics of ARs are projected to change in the future over the North Atlantic using 6-hourly output from the latest global climate model (GCM) simulations produced under CMIP5 [8]. These results are of paramount importance in gauging future changes in flooding over Britain and, by extension, much of northern and western Europe.

2. Data and methods

Five GCMs produced under CMIP5 [8] were considered in the analysis (supplementary table 1 available at stacks.iop.org/ERL/8/034010/mmedia) based on the availability of high time-resolution data (6-hourly model level diagnostics). For each model, four simulations were retrieved: Historical and AMIP (Atmospheric Model Intercomparison Project) runs

over 1980–2005 (1 October 1979–31 March 2005), and two future projection simulations (based on their availability) named representative concentration pathways (RCPs; RCP4.5 and RCP8.5 are labelled to reflect the radiative forcing change at the end of the 21st century, in W m^{-2}) assessed over 2074–2099 (1 October 2073–31 March 2099). The specific humidity (in kg kg^{-1}), and zonal and meridional winds (in ms^{-1}) were retrieved on model levels (and converted to pressure levels) at a 6-h resolution. We did not consider liquid and ice water since this typically comprises only a few % of the total column water mass within ARs, which is dominated by vapour. To establish realistic simulation of AR events, five atmospheric reanalyses (which use data assimilation of observations to provide the best three-dimensional dynamical representation of the atmosphere) were considered over the period 1980–2005: (1) Cooperative Institute for Research in Environmental Sciences (CIRES) Twentieth Century Reanalysis (20CR) [12]; (2) National Centers for Environmental Prediction (NCEP) Climate Forecast System Reanalysis (CFSR) [13]; (3) the European Centre for Medium-Range Weather Forecasts (ECMWF) ERA-Interim (ERAIN) [14]; (4) National Aeronautics and Space Administration (NASA)'s Modern Era Retrospective-analysis for Research and Applications (MERRA) [15]; and (5) NCEP–National Center for Atmospheric Research Reanalysis (NCEP–NCAR) [16]. The AMIP simulations prescribe observed sea surface temperature (SST) and sea-ice boundary conditions with a freely evolving atmosphere, and are used to evaluate whether Historical CMIP5 experiments (which simulate the fully coupled ocean–atmosphere system) are representative of actual conditions.

Research has identified spurious sources and sinks of moisture in a number of climate model simulations, although these are not unexpected and are in general small compared to precipitation and other fluxes in the global water cycle [17]. Pre-industrial control simulations of the MIROC5 and BCC-CSM-1 were affected by this issue to a greater extent than many other CMIP5 climate models [18]. Although potentially important in affecting atmospheric heating and associated feedbacks [17], we consider that our results are not significantly influenced by these inaccuracies because we do not use the pre-industrial control simulations and because potentially spurious moisture changes are negligible compared to physical changes driven by the Clausius–Clapeyron equation. Reanalysis simulations also suffer from imbalances in their global water cycle and spurious trends [19]. Again, these are only apparent when considering global mean changes and we consider that the detection of AR events in reanalyses is not substantially influenced by these limitations.

To detect ARs in the four simulations of the five selected CMIP5 models (and five reanalyses) we use the algorithm based on vertically integrated horizontal water vapour transport between 1000 and 300 hPa (herein, known as integrated vapour transport, IVT) developed in previous research [4]:

$$\text{IVT} = \sqrt{\left(\frac{1}{g}\int_{1000}^{300} qu\, \mathrm{d}p\right)^2 + \left(\frac{1}{g}\int_{1000}^{300} qv\, \mathrm{d}p\right)^2} \quad (1)$$

where q is the layer-averaged specific humidity in kg kg^{-1}, u and v are the layer-averaged zonal and meridional winds in ms^{-1} respectively, g is the acceleration due to gravity, and dp is the difference between adjacent model pressure levels (in hPa).

An IVT threshold was calculated for each model simulation ('model-dependent' threshold) and reanalysis thus reflecting different model climatologies. The IVT distribution in the region of interest (grid points spanning 50°N–60°N along 4°W) was computed by extracting the maximum IVT on all winter half-year days (at 1200UTC) for the 1980–2005 period, and the IVT value at the 85th percentile calculated (the 85th percentile approximately corresponds to the IVT value of the most intense ARs [4]). These IVT values were used to identify ARs affecting Britain. This procedure was repeated for each model and the CMIP5 models' IVT thresholds are shown in supplementary table 1. Note that a fixed IVT threshold corresponding to the median of all the models' and reanalyses' IVT thresholds was also used.

At each 6-h time step in the simulations over the winter half-year (over 1980–2005 and 2074–2099) the IVT was calculated at grid points spanning 50°N–60°N along approximately 4°W (note that 4°W roughly corresponds to landfall in western Britain). If the maximum IVT was greater than the model threshold (see supplementary table 1), the grid point was retained. When a grid point at 4°W was retained, the next step was to search adjacent grid points next to 4°W (to the northwest/south/southwest/west) for the highest IVT; the identified point was screened to determine if the IVT threshold was satisfied. This screening process was repeated across the North Atlantic, and if the IVT criterion was met at a specific number of grid points (as given by the number of grid points along a parallel for 20° longitude; i.e. number of grid points from 4°W to 24°W at one latitude), the time step was said to have an AR affecting Britain. Because the largest winter floods have been associated with spatiotemporally persistent AR events [3, 4], only ARs that occurred for three or more time steps (18 h or more), and only had a 4.5° latitude movement (during each consecutive 18-h period) to the north or south of the initial IVT maximum at 4°W between time steps were considered. Furthermore, to have independent events, two AR events were considered distinct only if they were separated by more than one day.

A sensitivity analysis was also employed to determine the thermodynamic contribution to future AR changes. For the Historical and RCP runs of each model, the average winter surface temperature (October to March over 1980–2005 and 2074–2099 respectively) over the North Atlantic Ocean (20°N–60°N; 60°W–0°) was calculated. The change in this regional temperature from the Historical to the RCPs was then used to artificially scale up the specific humidity accordingly in the Historical runs. This experiment effectively tests how many additional ARs would be detected over the model-dependent threshold if the Historical circulation pattern was combined with the increased water vapour expected from the increased temperature in the RCP simulations (specific humidity at low altitudes, where ARs are produced, increases by about 7% K^{-1} with warming [19]).

3. Results and discussion

Typical examples of ARs impacting Britain detected by our algorithm in the CMIP5 models' Historical runs (1980–2005) are shown in figure 1. The AR structures are qualitatively similar to those found in atmospheric reanalyses, as seen by the similarity with the ERA-Interim Reanalysis [14] (figure 1(f)). It is therefore evident that the CMIP5 models are capable of resolving AR-like structures, and thus the models are capable of capturing the relevant atmospheric mechanisms responsible for generating floods. In supplementary figure 1 (available at stacks.iop.org/ERL/8/034010/mmedia) we show histograms of the time span of the detected ARs in the five reanalyses and the five GCM historical runs. The results suggest that the models are generally capable of producing the persistent-type ARs that are observed in the real world.

Figure 2 shows time series of the number of winter ARs in the CMIP5 Historical and AMIP present-day simulations, and five observationally based atmospheric reanalyses (20CR [12], CFSR [13], ERAIN [14], MERRA [15], and NCEP–NCAR [16]). Many coupled climate models contain substantial SST biases (relative to observations) and, if the fixed IVT threshold method is used for AR detection, the models with the coldest SSTs in the North Atlantic (figure 2(g)) tend to have too few AR events in the Historical simulations (figure 2(h)—note particularly the CNRM and GFDL Historical simulations). This is consistent with the expectation that colder SSTs will be associated with colder near-surface air temperatures and, in consequence, reduced atmospheric water vapour content (typically 7% K^{-1}, as per the Clausius–Clapeyron relationship). However, the AMIP simulations which prescribe observed SST are able to represent the overall AR occurrence frequency well (when the fixed IVT Threshold is applied; figure 2(h)) albeit with a slight underestimation (∼5–10 ARs year^{-1} in CMIP5–AMIP compared to 9–11 ARs year^{-1} in reanalyses). As the use of a fixed IVT threshold leads to an underestimation in the Historical runs, an alternative approach to AR detection is adopted, whereby each model's climatology of ARs is used to define a model-dependent IVT threshold ('model-dependent' threshold). This approach thereby removes the cold-SST bias effect and it not only captures a larger number of ARs per year on average (see figure 2(f)), but the year-to-year variability is scaled appropriately (compare the grey line with the shaded areas in figures 2(a)–(e)).

After establishing that the CMIP5 Historical simulations are able (subject to a correction to remove a gross-scale temperature bias) to represent ARs in the present day, we can assess the projected changes in AR frequency and strength using future simulations. We focus on RCP4.5 and RCP8.5 and compare the AR projections for the period 2074–2099 with the corresponding Historical simulations (1980–2005). For all models there is an increase in AR frequency (figure 3—referring to the unhatched bars only) and a striking level of consistency on the magnitude of change in AR frequency amongst the models' RCP8.5 projections (all models have approximately double the number of ARs in RCP8.5 compared to Historical). Because of the established
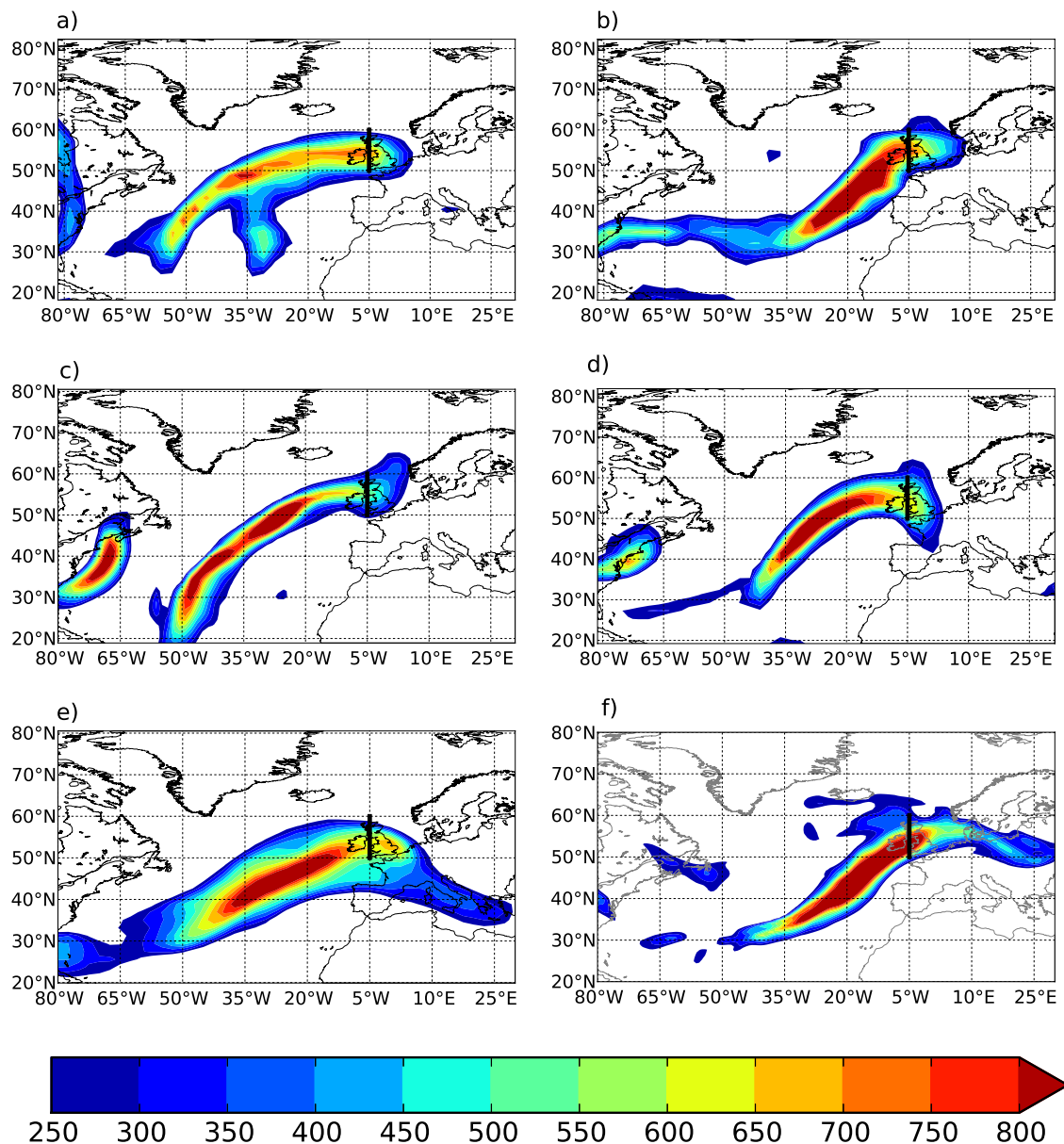
Figure 1. Maps of vertically integrated horizontal water vapour transport (IVT) at a 6-h time resolution in (a) bcc-csm1-1, (b) CanESM2, (c) CNRM-CM5, (d) GFDL-ESM2G, (e) NorESM1-M, and (f) ERAIN. The black line between 50°N and 60°N at about 4°W shows the region where the IVT is calculated. Units are kg m^{-1} s^{-1}.

link between ARs and heavy rainfall and flooding over Britain [3, 4], an increased AR frequency could result in an increased number of these potentially catastrophic flood events.

For each of the ARs identified in the Historical (1980–2005) and the RCP4.5 and RCP8.5 projections (2074–2099), the maximum IVT at 4°W (averaged over the lifetime of the AR) was calculated. Our results indicate that there is a projected increase in IVT in the future (see supplementary figure 2 available at stacks.iop.org/ERL/8/034010/mmedia). With an increase in radiative forcing and thus rising air temperatures, an increase in saturation vapour pressure and atmospheric moisture is expected in line with the Clausius–Clapeyron relationship. Therefore, an AR impacting Britain in the future is projected to deliver more moisture,

potentially causing larger precipitation totals and associated flooding. A two-sample Kolmogorov–Smirnov test (KS test) was applied to test whether the Historical IVT distributions were different from the RCP simulations. With the exception of the GFDL-ESM2G Historical versus RCP4.5, the null hypothesis that the distributions are the same is rejected at the 0.01 significance level.

The projected changes to the AR frequency and intensity could be due to a combination of dynamical and thermodynamic changes, including natural climate variability. The projected winter surface temperature rises (over the North Atlantic Ocean in the RCPs) used in the sensitivity analysis to characterize the thermodynamic component are shown in figure 3(f). A large proportion of the increase in AR frequency is explained by the thermodynamic scaling (figure 3; compare
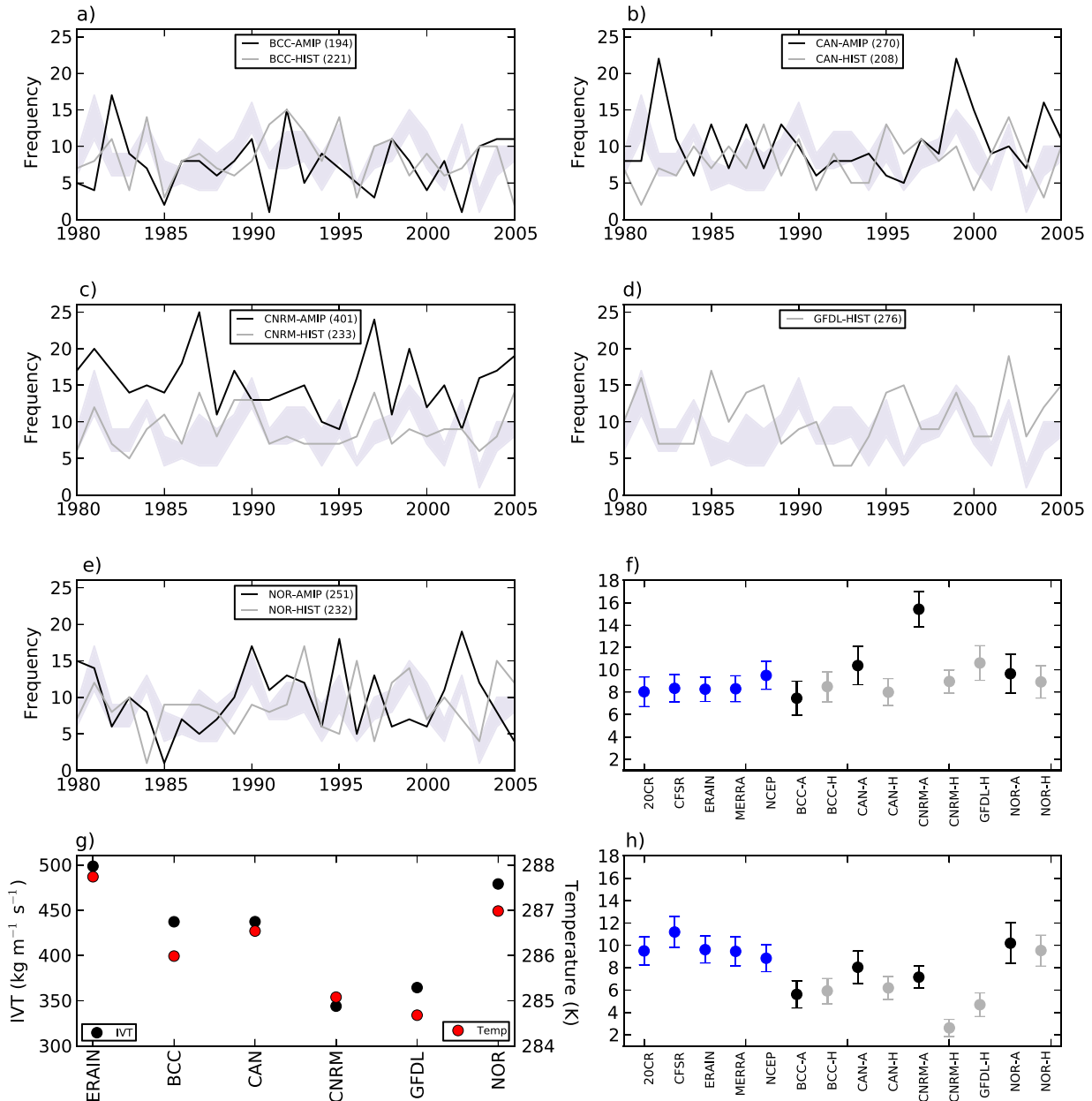
Figure 2. Time series of winter AR totals in the Historical (grey lines) and AMIP (black lines) runs in the (a) bcc-csm1-1 model, (b) CanESM2/AM4 model, (c) CNRM-CM5 model, (d) GFDL-ESM2G model, and (e) NorESM1-M model. The light blue shading represents the range of AR totals in the five reanalyses (20CR, CFSR, ERAIN, MERRA and NCEP–NCAR). Panel (f) contains the average number of ARs per winter (using a model-dependent IVT threshold) with the corresponding 2.5th–97.5th sampling confidence intervals (reanalyses are in blue). Panel (g) shows the average winter 2 m surface temperature (red points; right *y*-axis) over the North Atlantic region (20°N–60°N; 60°W–0°) and the IVT threshold (black points; left *y*-axis) from 1980 to 2005 for the CMIP5 models and ERAIN, and panel (h) shows the average number of ARs per winter (using a fixed IVT threshold) with the corresponding 2.5th–97.5th sampling confidence intervals (reanalyses are in blue).

the hatched bars with the equivalent unhatched bars). For the RCP4.5 sensitivity test there are some inconsistent signals: the thermodynamic scaling overestimates or underestimates the AR frequency change relative to the actual RCP4.5 simulations in different models (e.g., the scaling of the CNRM-CM5 and GFDL-ESM2G models explains about 50% of the increased AR activity compared to nearly 100% for the CanESM2). In all RCP4.5 cases, however, a large proportion of the response is accounted for by this simple thermodynamic scaling. In the RCP8.5, the thermodynamic component always

underestimates the actual RCP8.5 results, but again the thermodynamic component explains 50% or more of the total change. The remaining changes in AR activity are therefore likely to be due to a dynamical component (spatial movement of storm tracks [9] and their variability [20]), with natural variability of the climate system also contributing because of the 26-year time slices analysed.

To further evaluate the origin of the change in AR intensity, scatterplots of the average low-level (about 900 hPa) specific humidity and winds during the detected ARs (at 4°W
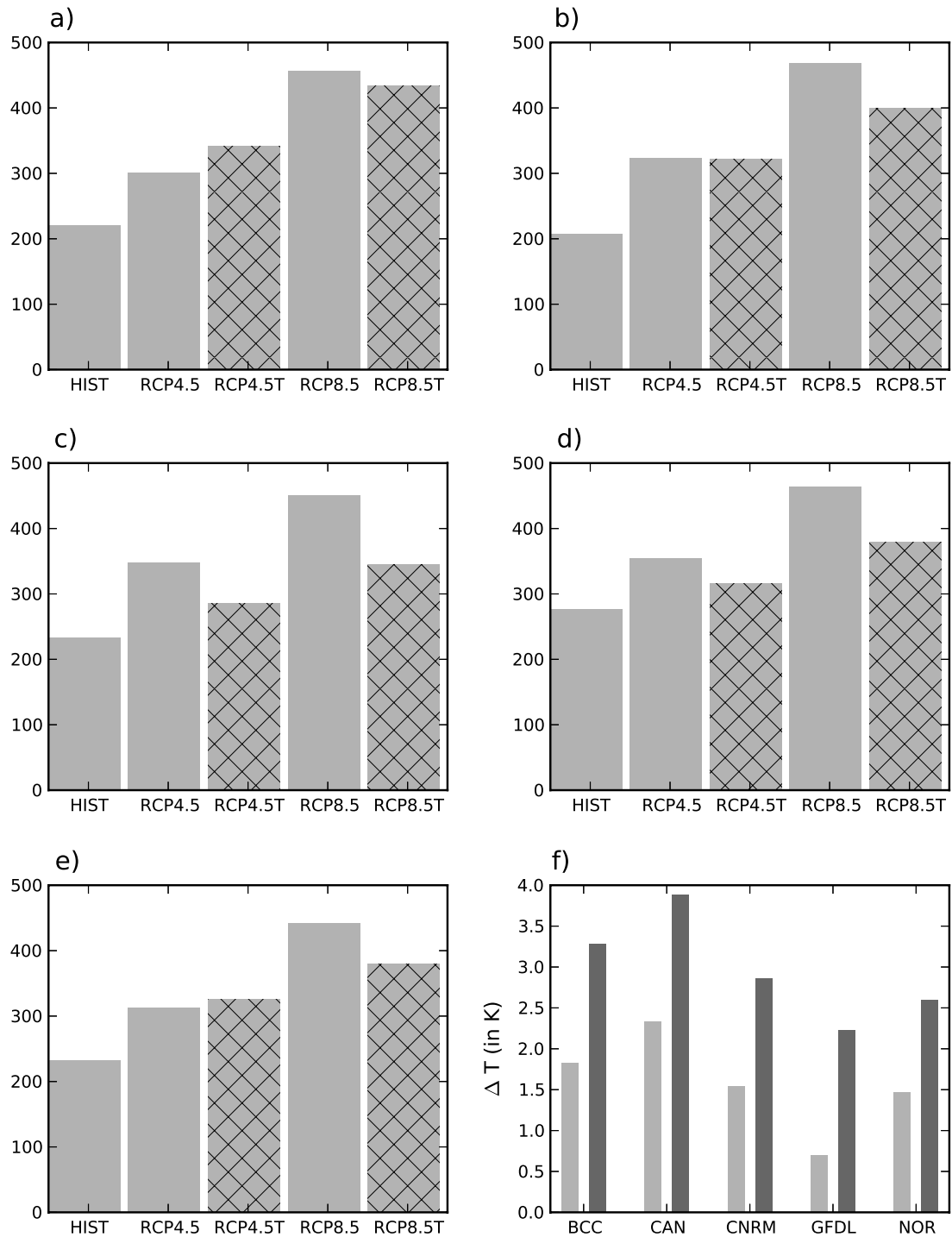
Figure 3. The total number of winter ARs in the Historical, RCP4.5, RCP8.5, and the scaled up Historical runs (RCP4.5T and RCP8.5T; hatched bars) in the (a) bcc-csm1-1, (b) CanESM2, (c) CNRM-CM5, (d) GFDL-ESM2G and (e) NorESM1-M. Panel (f) shows the rise in North Atlantic surface temperature (20°N–60°N; 60°W–0°) in the RCPs compared to the Historical runs; light grey is RCP4.5 and dark grey is RCP8.5.

over the AR lifetime) for the Historical and RCP4.5, and Historical and RCP8.5 simulations were generated (figure 4 for NorESM1-M Historical and RCP8.5 runs; the other models are shown in the supplementary material available at stacks.iop.org/ERL/8/034010/mmedia). Here, the same number of AR events is used in the Historical and RCP4.5 and RCP8.5 scatterplots (i.e., if 200 ARs occurred in the

Historical run, then only the 200 largest ARs in RCP8.5 in terms of IVT were selected). Using this approach, we can isolate changes in the characteristics of the most intense ARs. Crucially, the future low-level specific humidity distributions of the ARs appear to have shifted towards increased values compared to the past (figure 4, right-hand side panel). There is, however, little evidence for a shift in the distributions of the
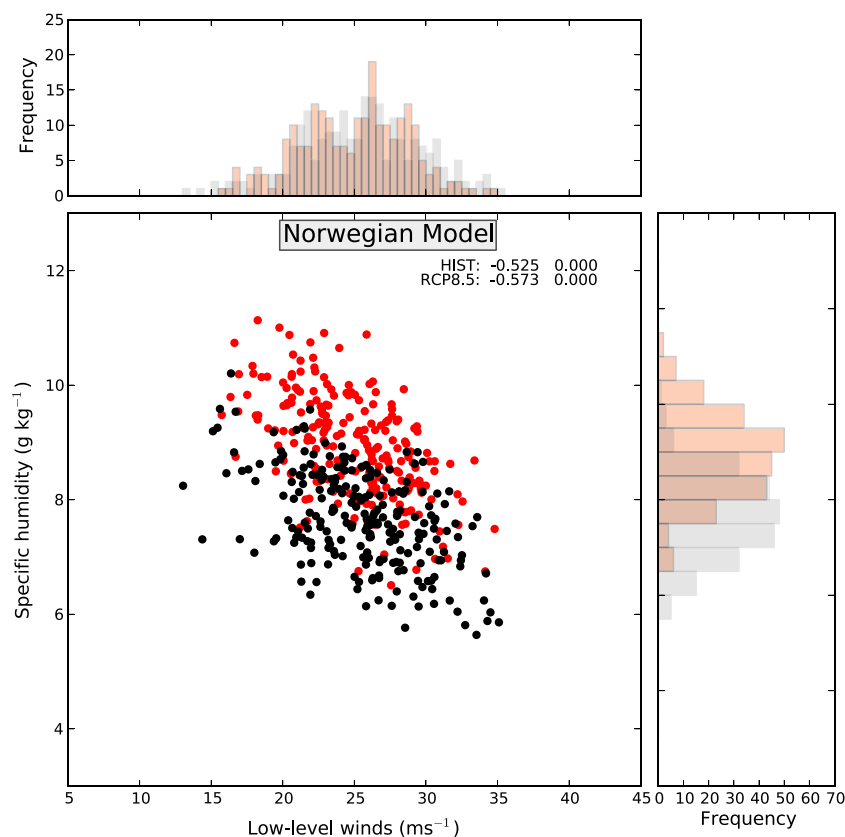
Figure 4. Scatterplot of the low-level winds (ms^{-1}) versus the low-level specific humidity (g kg^{-1}) in the Historical (black) and RCP8.5 (red) runs of the NorESM1-M model. Histograms of the marginal distributions are shown, highlighting the shift in the specific humidity distribution. The Pearson product moment correlation coefficient (left) and *p*-value (right) between the low-level winds and specific humidity is shown for the historical and RCP8.5 scenarios.

winds in this model (figure 4, top panel) consistent with the thermodynamic-related effects dominating in this model. This is confirmed by KS test results, which show that the future specific humidity distributions are different from the historical distributions at the 0.01 significance level, whereas none of the low-level wind distributions is significantly different. This result is consistent across all models in both RCP4.5 and RCP8.5 simulations (see supplementary material) suggesting that the increasing IVT in the future is largely due to increased moisture in the atmosphere, thus corroborating the sensitivity test that the increased AR frequency is thermodynamically driven.

4. Conclusions

Our analysis demonstrates that under current climate change scenarios, the strongest ARs are projected to become more intense and—for any given intensity threshold— more frequent, indicating an intensification of precipitation extremes [6, 19]. A large part of these changes is thermodynamic in origin, suggesting that they are a relatively robust response to anthropogenic climate forcing. We conclude that peak multi-day precipitation totals associated with extra-tropical cyclones could intensify over Britain, with more frequent and larger winter flood episodes as a result. The results presented are not only regionally relevant, but

are likely to apply more widely to Western Europe as ARs are also a feature behind extreme precipitation here [5]. Our study provides a framework for the examination of potential AR changes in other mid-latitude regions and highlights a useful tool for directly examining the atmospheric features most relevant to mid-latitude winter flooding in atmospheric models. Furthermore, the research undertaken has policy relevance, as the monitoring and reporting of changes in AR activity could be used to evaluate future extreme flood risk, especially in areas of upland Britain.

References

[1] Ralph F M, Neiman P J, Wick G A, Gutman S I, Dettinger M D, Cayan D R and White A B 2006 Flooding on California's Russian river: role of atmospheric rivers *Geophys. Res. Lett.* **33** L13801

[2] Neiman P J, Schick L J, Ralph F M, Hughes M and Wick G A 2011 Flooding in western Washington: the connection to atmospheric rivers *J. Hydrometeorol.* **12** 1337–58

[3] Lavers D A, Allan R P, Wood E F, Villarini G, Brayshaw D J and Wade A J 2011 Winter floods in Britain are connected to atmospheric rivers *Geophys. Res. Lett.* **38** L23803

[4] Lavers D A, Villarini G, Allan R P, Wood E F and Wade A J 2012 The detection of atmospheric rivers in atmospheric reanalyses and their links to British winter floods and the large-scale climatic circulation *J. Geophys. Res.* **117** D20106

[5] Lavers D A and Villarini G 2013 The nexus between atmospheric rivers and extreme precipitation across Europe *Geophys. Res. Lett.* **40** 3259–64

[6] Held I M and Soden B J 2006 Robust responses of the hydrological cycle to global warming *J. Clim.* **19** 5686–99

[7] Dettinger M 2011 Climate change, atmospheric rivers, and floods in California—a multimodel analysis of storm frequency and magnitude changes *J. Am. Water Resour. Assoc.* **47** 514–23

[8] Taylor K E, Stouffer R J and Meehl G A 2012 An overview of CMIP5 and the experiment design *Bull. Am. Meteorol. Soc.* **93** 485–98

[9] Zappa G, Shaffrey L C, Hodges K I, Sansom P G and Stephenson D B 2013 A multi-model assessment of future projections of North Atlantic and European extratropical cyclones in the CMIP5 climate models *J. Clim.* at press (doi:10.1175/JCLI-D-12-00573.1)

[10] Ulbrich U, Pinto J G, Kupfer H, Leckebusch G C, Spangehl T and Reyers M 2008 Changing northern hemisphere storm tracks in an ensemble of IPCC climate change simulations *J. Clim.* **21** 1669–79

[11] Yin J H 2005 A consistent poleward shift of the storm tracks in simulations of 21st century climate *Geophys. Res. Lett.* **32** L18701

[12] Compo G P *et al* 2011 The twentieth century reanalysis project *Q. J. R. Meteorol. Soc.* **137** 1–28

[13] Saha S *et al* 2010 The NCEP climate forecast system reanalysis *Bull. Am. Meteorol. Soc.* **91** 1015–57

[14] Dee D P *et al* 2011 The ERA-Interim reanalysis: configuration and performance of the data assimilation system *Q. J. R. Meteorol. Soc.* **137** 553–97

[15] Rienecker M M *et al* 2011 MERRA: NASA's modern-era retrospective analysis for research and applications *J. Clim.* **24** 3624–48

[16] Kalnay E *et al* 1996 The NCEP/NCAR 40-year reanalysis project *Bull. Am. Meteorol. Soc.* **77** 437–71

[17] Liepert B G and Previdi M 2012 Inter-model variability and biases of the global water cycle in CMIP3 coupled climate models *Environ. Res. Lett.* **7** 014006

[18] Liepert B G and Lo F 2013 CMIP5 update of 'Inter-model variability and biases of the global water cycle in CMIP3 coupled climate models' *Environ. Res. Lett.* **8** 029401

[19] Allan R P, Liu C, Zahn M, Lavers D A, Koukouvagias E and Bodas-Salcedo A 2013 Physically consistent responses of the global atmospheric hydrological cycle in models and observations *Surv. Geophys.* doi:10.1007/s10712-012-9213-z

[20] Harvey B J, Shaffrey L, Woollings T, Zappa G and Hodges K I 2012 How large are projected 21st century storm track changes? *Geophys. Res. Lett.* **39** L18707